

PAPER • OPEN ACCESS

## Hydroisomerization of n-hexadecane over H $\beta$ molecular sieve loading palladium bifunctional catalyst: effect of SiO<sub>2</sub>/Al<sub>2</sub>O<sub>3</sub> molar ratios

To cite this article: X F Bai *et al* 2019 *IOP Conf. Ser.: Mater. Sci. Eng.* **504** 012042

View the [article online](#) for updates and enhancements.

## Hydroisomerization of n-hexadecane over H $\beta$ molecular sieve loading palladium bifunctional catalyst: effect of SiO<sub>2</sub>/Al<sub>2</sub>O<sub>3</sub> molar ratios

X F Bai<sup>1,2</sup>, X M Wei<sup>2</sup>, Y Liu<sup>1</sup> and W Wu<sup>2</sup>

<sup>1</sup>Institute of Petrochemistry, Heilongjiang Academy of Sciences, Harbin 150040, China

<sup>2</sup>School of Chemistry and Material Sciences, Heilongjiang University, Harbin 150080, China

Corresponding author and e-mail: W Wu, marywu64@126.com

**Abstract.** H $\beta$  molecular sieves with different SiO<sub>2</sub>/Al<sub>2</sub>O<sub>3</sub> ratios (H $\beta$ (x)) and H $\beta$ (x) loading Pd(0.5 wt%) bifunctional catalysts (Pd/H $\beta$ (x)) were prepared by hydrothermal synthesis and incipient wetness impregnation, respectively. The structure, morphology, pore and acid properties of H $\beta$ (x) and Pd dispersion of Pd/H $\beta$ (x) were characterized using XRD, SEM, N<sub>2</sub> physical adsorption, NH<sub>3</sub>-TPD and H<sub>2</sub> chemical absorption. H $\beta$ (x) samples were highly crystalline microporous materials. With the increase of SiO<sub>2</sub>/Al<sub>2</sub>O<sub>3</sub> ratios, BET surface area, micro-pore surface area and volume of H $\beta$ (x) gradually decreased, and the external surface area and mesoporous volume gradually increased, and the number and acid strength of weak acid sites for H $\beta$ (x) and Pd dispersion for Pd/H $\beta$ (x) decreased. It was known from hydroisomerization performance of n-C<sub>16</sub>H<sub>34</sub> that Pd/H $\beta$ (40) catalysts showed the highest conversion of 96.9% at 230 °C. The selectivity of iso-C<sub>16</sub>H<sub>34</sub> reached the highest value at the n-C<sub>16</sub>H<sub>34</sub> conversion of 45~50%. Pd/H $\beta$ (40) catalysts exhibited the highest iso-C<sub>16</sub>H<sub>34</sub> selectivity of 84.4%, much more multi-branched iso-C<sub>16</sub>H<sub>34</sub> and C<sub>4</sub>+C<sub>5</sub> cracking components. The decrease of SiO<sub>2</sub>/Al<sub>2</sub>O<sub>3</sub> molar ratios can increase the number of acid sites and dispersion of Pd/H $\beta$ (x) bifunctional catalysts, thus not only aggravating the secondary heterogeneous reaction, but also accelerating the serious secondary cracking reaction.

### 1. Introduction

Biodiesel is a kind of renewable, efficient and safe clean energy, which has been greatly developed in recent years[1]. Hydroisomerization of deoxygenated oil is an important means to improve the hexadecane value and low temperature fluidity of biodiesel[2~3]. In hydroisomerization reaction process, the cracking reaction of the long carbon chain alkanes will produce light hydrocarbon component content, which reduce the selectivity of alkane isomer and liquid yield of diesel fuel[4~5]. It is the key to develop efficient catalysts for hydroisomerization reactions to suppress cracking reaction on the basis of good catalytic activity[6].

The acidity of the bifunctional catalyst obtained by using molecular sieve as acid carrier will directly influence the reaction activity and the selectivity of the isomerized product of long carbon chain n-alkanes hydroisomerization [7~8].

Herein, H $\beta$  molecular sieves with four different SiO<sub>2</sub>/Al<sub>2</sub>O<sub>3</sub> ratios were hydrothermally synthesized



and Pd/H $\beta$  bifunctional catalysts were prepared by incipient wetness impregnation. Pd/H $\beta$  catalysts were used for hydroisomerization of n-hexadecane. The effect of SiO<sub>2</sub>/Al<sub>2</sub>O<sub>3</sub> ratios on the physicchemical properties of H $\beta$  and Pd/H $\beta$ , its catalytic hydroisomerization performance was investigated.

## 2. Experimental section

### 2.1. Preparation of H $\beta$ molecular sieves with different SiO<sub>2</sub>/Al<sub>2</sub>O<sub>3</sub> ratios and loading palladium bifunctional catalysts

H $\beta$  molecular sieves were hydrothermally synthesized using NaAlO<sub>2</sub> (CP, Sinopharm chemical reagent co. LTD), ludox (26.85 wt% SiO<sub>2</sub>, Qingdao Yumin Company, China) and tetraethylammonium hydroxide (CP, Sinopharm chemical reagent Co. LTD) as Al source, Si source and template agent, respectively. The molar ratio of the initial gel was 1SiO<sub>2</sub>:*n*Al<sub>2</sub>O<sub>3</sub>:0.05B<sub>2</sub>O<sub>3</sub>:0.22TEAOH:0.025NaOH:0.05Na<sup>+</sup>:18 H<sub>2</sub>O (*n* = 0.025~ 0.01). The synthesis process was as follows: NaAlO<sub>2</sub>, TEAOH, H<sub>3</sub>BO<sub>3</sub> and ludox were in turn added to secondary deionized water, stirred well, transferred into a crystallization autoclave lined with Teflon, and hydrothermally crystallized at 145 °C for 5 days. The crystallization products were separated by centrifugation, dried at 110 °C, calcined at 560 °C to remove the template. The above-prepared molecular sieves were referred to as Na $\beta$ (*x*), where *x* is the SiO<sub>2</sub>/Al<sub>2</sub>O<sub>3</sub> molar ratio (*x* = 40, 60, 80 and 100). Na $\beta$ (*x*) were treated by 0.5 mol/L NH<sub>4</sub>NO<sub>3</sub> solution at 70 °C, then dried and roasted to obtain H $\beta$ (*x*) molecular sieves. H $\beta$ (*x*) loading Pd(0.5wt%) bifunctional catalysts (Pd/H $\beta$ (*x*)) were prepared by incipient wetness impregnation with a Pd(NO<sub>3</sub>)<sub>2</sub> solution.

### 2.2. Characterization of H $\beta$ (*x*) and Pd/H $\beta$ (*x*) catalysts

X-ray diffraction (XRD) patterns of H $\beta$ (*x*) were measured on a Bruker D8 Advance diffractometer with a Cu K $\alpha$  radiation ( $\lambda$  = 0.154 nm). The morphology of H $\beta$ (*x*) was performed by scanning electronic microscopy (SEM) on a FEI Sirion microscope. The N<sub>2</sub> absorption and desorption isotherms were carried out using an Autosorb-iQ2 apparatus (Quantachrome Instruments). The surface area and pore volume were calculated according to BET method and the t-plot method, respectively. The acid sites of H $\beta$ (*x*) was measured by NH<sub>3</sub> temperature-programmed desorption (NH<sub>3</sub>-TPD) on a conventional set-up equipped with a thermal conductivity detector (TCD). The Pd dispersion of Pd/H $\beta$ (*x*) was determined by H<sub>2</sub> chemical absorption analysis using an AutoChem II 2920 Chemisorption Analyzer.

### 2.3 Catalytic hydroisomerization of n-hexadecane

The catalytic hydroisomerization of n-hexadecane (n-C<sub>16</sub>H<sub>34</sub>) were carried out in a fixed-bed reactor. Firstly, 1.0 g Pd/H $\beta$ (*x*) were reduced in situ with H<sub>2</sub> at 400 °C for 1 h. Then, the catalyst was cooled to the reaction temperature, and H<sub>2</sub>/n-C<sub>16</sub>H<sub>34</sub> were fed into the reactor at a pressure of 2.0 MPa, a H<sub>2</sub>/n-C<sub>16</sub>H<sub>34</sub> of 8.72 (molar ratio) and WHSV of 3.70 h<sup>-1</sup>. The composition of products after reacting for 2 h was analyzed using a GC (Agilent 6820) with a HP-1 (60 m\*0.25 mm\*1.00  $\mu$ m) capillary column and a FID detector.

## 3. Results and discussion

### 3.1. The characterization of H $\beta$ (*x*) and Pd/H $\beta$ (*x*) with different SiO<sub>2</sub>/Al<sub>2</sub>O<sub>3</sub> ratios

#### 3.1.1. XRD

The XRD patterns of H $\beta$ (*x*) with different SiO<sub>2</sub>/Al<sub>2</sub>O<sub>3</sub> molar ratios are shown in Figure 1. The diffraction peaks at 7.7°, 21.5°, 22.7°, 27.1°, 29.7°, which are exclusively attributed to  $\beta$  topological structure, can be observed for H $\beta$ (*x*) with different SiO<sub>2</sub>/Al<sub>2</sub>O<sub>3</sub> molar ratios. There were no additional peaks to be observed in the spectral patterns, indicating that the above-synthesized H $\beta$ (*x*) molecular

sieves were free from impurities. The high intensity of the XRD peaks indicated that  $H\beta(x)$  with different  $SiO_2/Al_2O_3$  molar ratios were highly crystalline materials.

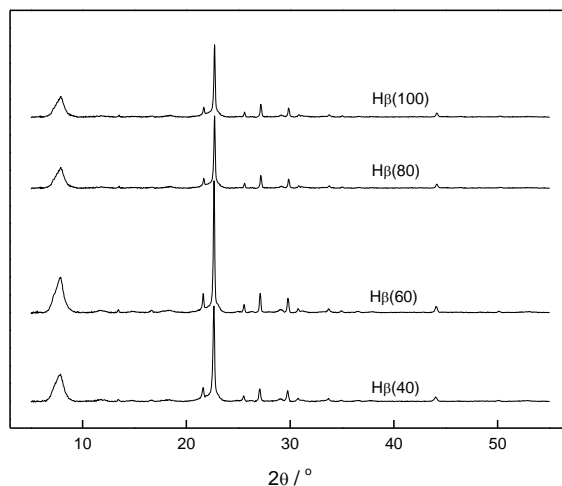


**Figure 1.** XRD patterns of  $H\beta(x)$  samples.

### 3.1.2. SEM

Figure 2 shows the SEM images of  $H\beta(x)$  samples with different  $SiO_2/Al_2O_3$  molar ratios.

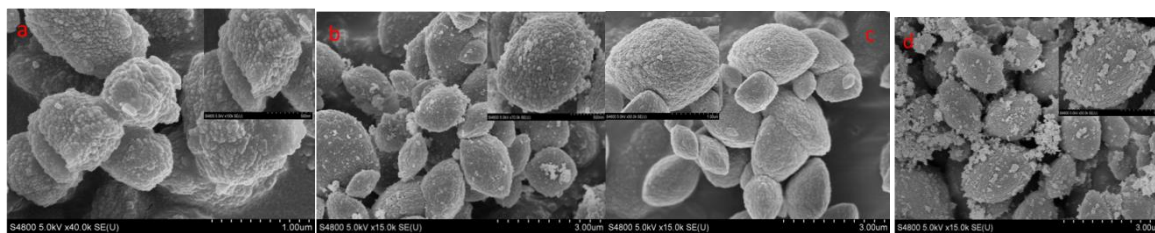


**Figure 2.** SEM images of  $H\beta(x)$  samples: a.  $x=40$ ; b.  $x=60$ ; c.  $x=80$ ; d.  $x=100$ .

It can be seen from Figure 2 that the as-synthesized  $H\beta(x)$  samples present elliptic spherical morphology stacked by nano sheet with the thickness of 100~300 nm, which is the typical structure of  $\beta$  molecular sieves. In addition, the size of the  $H\beta(x)$  aggregates is between 1.5~3 $\mu m$  and not significantly different with the increase of  $SiO_2/Al_2O_3$  ratios. There are distinct irregular granular aggregates on its surface of  $H\beta(100)$ , which may be due to the formation of some non-skeleton species.

### 3.1.3. $N_2$ physical adsorption

$N_2$  adsorption-desorption isotherms of  $H\beta(x)$  samples with different  $SiO_2/Al_2O_3$  molar ratios are shown in Figure 3 to specify the pore structure. The specific surface area and pore volume of all samples are listed in Table 1.

As shown in Figure 3, the dsorption-desorption isotherms of all  $H\beta(x)$  samples are corresponding to a type I isotherm, which indicating that as-synthesized  $H\beta(x)$  molecular sieves are microporous materials. A hysteresis loop appears at a relatively high partial pressure, which indicating the existence of mesoporous structure in  $H\beta(x)$ .

As can be seen from Table 1, with the increase of  $SiO_2/Al_2O_3$  molar ratio in the crystallization products, BET surface area, micro-pore surface area and volume of all  $H\beta(x)$  samples gradually decreased, and the external surface area and mesoporous volume gradually increased. This may be due

to the increase of Si source adding amount in the initial gel, the reduction of the reaction rate of depolymerization and condensation polymerization of silicon atoms in the gel may lead to more defect sites in the skeleton.

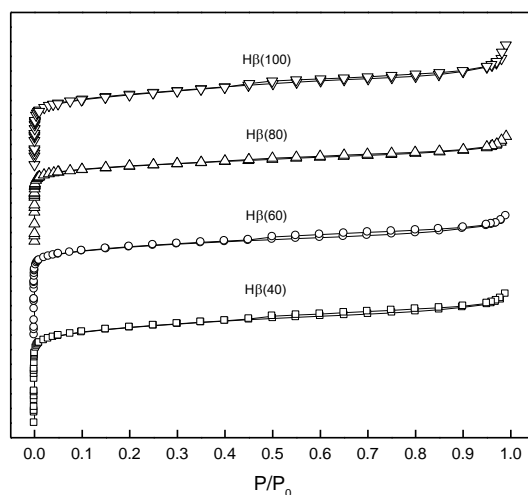


**Figure 3.** N<sub>2</sub> adsorption-desorption isotherm of Hβ(x) samples.

**Table 1.** N<sub>2</sub> physical adsorption data of Hβ(x) samples.

Sample	Surface area(m <sup>2</sup> /g)			Pore volume (cm <sup>3</sup> /g)		
	BET	Micropore	External	Total	Micropore	Mesopore
Hβ(40)	648	545	103	0.341	0.216	0.125
Hβ(60)	614	527	87	0.314	0.196	0.118
Hβ(80)	591	507	84	0.277	0.162	0.115
Hβ(100)	553	432	121	0.271	0.146	0.125

<sup>a</sup> BET method, <sup>b</sup> t-plot method, <sup>c</sup> Volume adsorbed at  $p/p_0 = 0.99$

### 3.1.4. NH<sub>3</sub>-TPD

In order to investigate the effect of SiO<sub>2</sub>/Al<sub>2</sub>O<sub>3</sub> molar ratio on the acid strength and acid amount of molecular sieve, as-synthesized Hβ(x) samples were characterized by NH<sub>3</sub>-TPD shown in Figure 4 and Table 2.

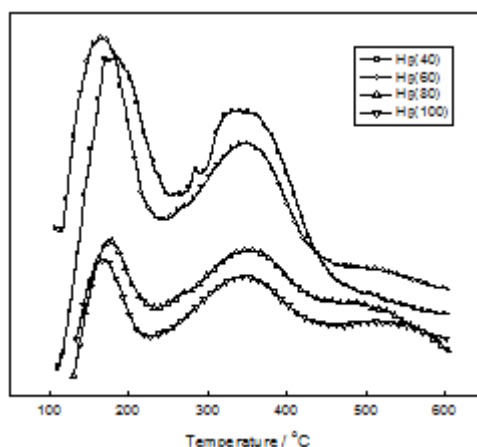


**Figure 4.** NH<sub>3</sub>-TPD profiles of Hβ(x) samples.

**Table 2.** Acid datas of H $\beta$ (x) samples.

Sample	Acid amount (mmol/g)			T/°C	
	Weak	Strong	Total	LT	HT
H $\beta$ (40)	0.40	0.45	0.85	180	346
H $\beta$ (60)	0.46	0.37	0.83	163	345
H $\beta$ (80)	0.21	0.37	0.58	176	346
H $\beta$ (100)	0.17	0.32	0.49	165	345

As can be seen from Figure 4, two peaks of ammonia desorption appear in the NH<sub>3</sub>-TPD graphs of each sample. The peaks at 163~180 °C, 345~346 °C are assigned to the ammonia desorbed from the weak and strong acid sites, respectively. It can be seen from the data in Table 2 that with the increase of SiO<sub>2</sub>/Al<sub>2</sub>O<sub>3</sub> molar ratios (especially more than 60), the acid strength and the number of weak acid sites obviously decrease, but the acid strength of strong acid sites remained basically unchanged and the number of strong acid sites decreased slightly.

### 3.1.5. H<sub>2</sub> chemical absorption

Pd/H $\beta$ (x) bifunctional catalysts were characterized by H<sub>2</sub> chemical adsorption analysis to investigate the effect the SiO<sub>2</sub>/Al<sub>2</sub>O<sub>3</sub> molar ratios on Pd dispersion shown in Table 3.

**Table 3.** Metal Pd dispersion and sites of Pd/ H $\beta$ (x) catalysts.

Catalysts	Metal dispersion (%)	C <sub>Pd</sub> (μmol/g)
Pd/H $\beta$ (40)	47.6	22.4
Pd/ H $\beta$ (60)	33.1	15.6
Pd/ H $\beta$ (80)	31.4	14.8
Pd/ H $\beta$ (100)	27.8	13.2

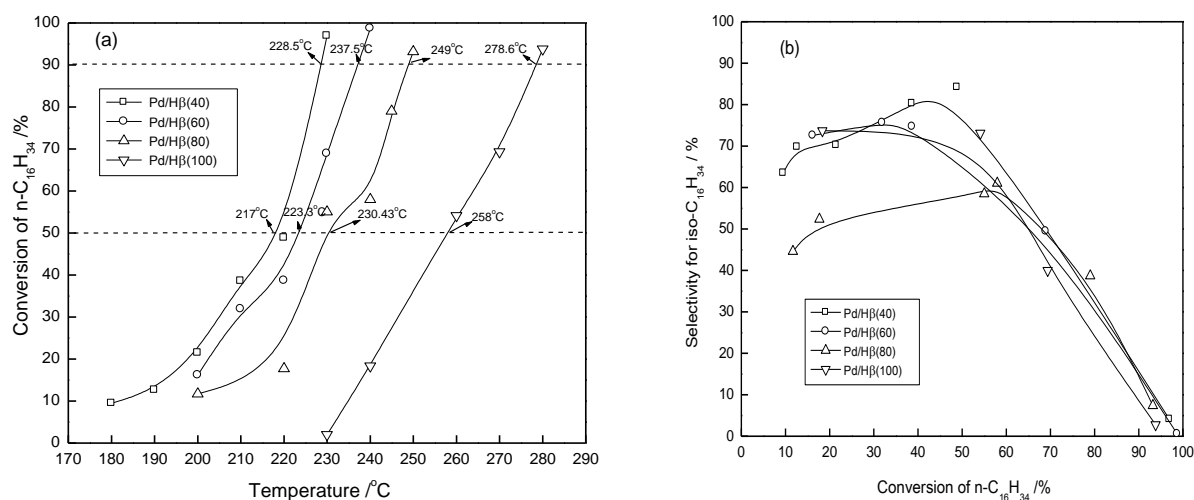
It can be seen from the data in Table 3 that Pd dispersion on Pd/H $\beta$ (x) bifunctional catalysts is proportional to the amount of H $\beta$ (x) strong acid, which indicates that the lower SiO<sub>2</sub>/Al<sub>2</sub>O<sub>3</sub> molar ratios is helpful to the dispersion of metal particles on surface of H $\beta$ (x).

### 3.2. Effect of SiO<sub>2</sub>/Al<sub>2</sub>O<sub>3</sub> ratios on catalytic hydroisomerization performace of *n*-hexadecane over Pd/H $\beta$ (x) bifunctional catalysts

The hydroisomerization of *n*-hexadecane (n-C<sub>16</sub>H<sub>34</sub>) over Pd/H $\beta$ (x) bifunctional catalysts was carried out to investigate the effect of SiO<sub>2</sub>/Al<sub>2</sub>O<sub>3</sub> ratios on catalytic performance, and the results were shown in Figure 5~6.

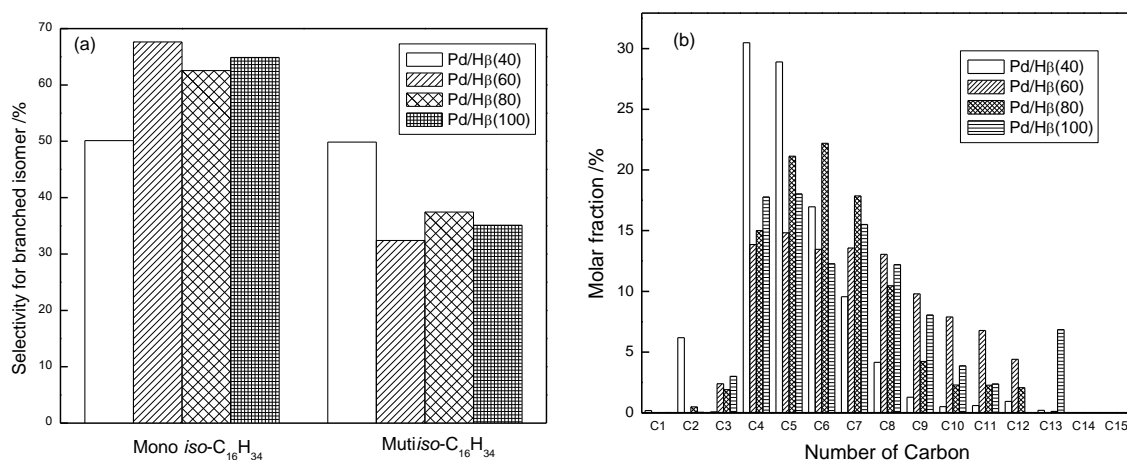
It can be seen from Figure 5(a) that the hydroisomerization reaction temperature rises with the increase of SiO<sub>2</sub>/Al<sub>2</sub>O<sub>3</sub> ratios under the condition of the same conversion rate of *n*-C<sub>16</sub>H<sub>34</sub>, indicating that the smaller the SiO<sub>2</sub>/Al<sub>2</sub>O<sub>3</sub> ratios, the higher the catalytic activity of Pd/H $\beta$ (x) catalysts is. This is because the acid site density and Pd dispersion decreased with the increase of SiO<sub>2</sub>/Al<sub>2</sub>O<sub>3</sub> ratios for Pd/H $\beta$ (x) catalysts. The catalytic activity in the hydroisomerization of *n*-C<sub>16</sub>H<sub>34</sub> decreased in the following order: Pd/H $\beta$ (40) > Pd/H $\beta$ (60) > Pd/H $\beta$ (80) > Pd/H $\beta$ (100). Pd/H $\beta$ (40) catalysts showed the highest conversion of *n*-C<sub>16</sub>H<sub>34</sub> of 96.9% at the temperature of 230 °C.

Figure 5(b) shows the relationship between the selectivity of iso-C<sub>16</sub>H<sub>34</sub> and conversion of *n*-C<sub>16</sub>H<sub>34</sub> over Pd/H $\beta$ (x). The selectivity of isomer products over the four Pd/H $\beta$ (x) catalysts presented a trend of first increasing and then decreasing with the increase of conversion. The selectivity of iso-C<sub>16</sub>H<sub>34</sub> reached the highest value at the *n*-C<sub>16</sub>H<sub>34</sub> conversion of 45~50%, and then went down fast with the further increase of conversion. Among four kinds of Pd/H $\beta$ (x) bifunctional catalysts, Pd/H $\beta$ (40) catalysts showed the highest selectivity of 84.4%. This is mainly because Pd/H $\beta$ (40) bifunctional catalyst is of the highest acid site density and Pd dispersion, which may lower the reaction temperature, thus reducing the low probability of cracking reaction.



**Figure 5.** Catalytic performance of  $n\text{-C}_{16}\text{H}_{34}$  hydroisomerization over Pd/H $\beta$ (x) catalysts. (a) Conversion of  $n\text{-C}_{16}\text{H}_{34}$ ; (b) Selectivity for  $iso\text{-C}_{16}\text{H}_{34}$ ;

Figure 6 shows the product distribution of mono-branched  $iso\text{-C}_{16}\text{H}_{34}$  and multi-branched  $iso\text{-C}_{16}\text{H}_{34}$  at the highest selectivity of  $iso\text{-C}_{16}\text{H}_{34}$  and the distribution of cracking products at  $n\text{-C}_{16}\text{H}_{34}$  conversion of 50%, respectively.



**Figure 6.** Distribution of products over Pd/H $\beta$ (x) catalysts (a) distribution of Mono  $iso\text{-C}_{16}\text{H}_{34}$  and Multi  $iso\text{-C}_{16}\text{H}_{34}$  at the high selectivity of  $iso\text{-C}_{16}\text{H}_{34}$ ; (b) distribution of cracking product at  $n\text{-C}_{16}\text{H}_{34}$  conversion of 50%.

It can be seen from Figure 6(a) that the amount of multi-branched  $iso\text{-C}_{16}\text{H}_{34}$  over Pd/H $\beta$ (40) was much higher than that over the other three Pd/H $\beta$ (x), which was due to the more number of acid sites and higher Pd dispersion of Pd/H $\beta$ (40) to aggravate the secondary heterogeneous reaction. At the same time, the serious secondary cracking reaction also occurred and the amount of C4 and C5 components was much more than the amount of C8 components in the hydroisomerization of  $n\text{-C}_{16}\text{H}_{34}$  over Pd/H $\beta$ (40) compared with the other three Pd/H $\beta$ (x), as shown in Figure 6(b).

#### 4. Conclusions

In summary, H $\beta$  molecular sieves with different  $\text{SiO}_2/\text{Al}_2\text{O}_3$  molar ratios (H $\beta$ (x)) were successfully

synthesized by hydrothermal synthesis and H $\beta$ (x) loading palladium bifunctional catalysts(Pd/H $\beta$ (x)) were prepared by incipient wetness impregnation. H $\beta$ (x) samples were highly crystalline microporous materials with the existence of mesoporous structure and free from impurities. With the increase of SiO<sub>2</sub>/Al<sub>2</sub>O<sub>3</sub> ratios, the size of the H $\beta$ (x) aggregates stacked by nano sheet is not significantly different, but BET surface area, micro-pore surface area and micro-pore volume of H $\beta$ (x) samples gradually decreased, and the external surface area and mesoporous volume gradually increased, and the acid strength and the number of weak acid sites for H $\beta$ (x) and Pd dispersion for Pd/H $\beta$ (x) decreased. Pd/H $\beta$ (40) catalysts showed the highest conversion of n-hexadecane of 96.9% at the temperature of 230 °C. The selectivity of iso-C<sub>16</sub>H<sub>34</sub> reached the highest value at the n-C<sub>16</sub>H<sub>34</sub> conversion of 45~50%, and then went down fast with the further increase of conversion. Pd/H $\beta$ (40) catalysts exhibited the highest iso-C<sub>16</sub>H<sub>34</sub> selectivity of 84.4%, much more multi-branched *iso*-C<sub>16</sub>H<sub>34</sub> and C4&C5 cracking components. The following conclusions can be obtained from the experimental results that the lower SiO<sub>2</sub>/Al<sub>2</sub>O<sub>3</sub> molar ratios can increase the number of acid sites and dispersion of Pd/H $\beta$ (x) bifunctional catalysts, thus not only aggravating the secondary heterogeneous reaction, but also accelerating the serious secondary cracking reaction.

### Acknowledgements

This work was financially supported by National Natural Science Foundation of China (No. 21676074), Project of Heilongjiang Science and technology (Grant No. ZY17A06) and Science Foundation of Heilongjiang Academy of Sciences (Grant No. YY2017SH01& ZNBZ2018SH01).

### References

- [1] Gerhard K, Luis F R 2017 *Progress in Energy and Combustion Science* 58 36
- [2] Luis C G , Danielle O R, Rodrigo C C ,et al 2017 *Fuel* 209 521
- [3] William P, James M, Juan R, et al 2017 *Fuel* 209 442
- [4] Liu S, Ren J, Zhang H, et al 2016 *Journal of Catalysis* 335 11
- [5] Kim M Y, Lee K, Choi M 2014 *Journal of Catalysis* 319 232
- [6] Zhang J W, Wu H M, Zhao A J 2017 *J Porous Mater* 24 437
- [7] Song X M, Bai X F, Wu W 2017 *Molecular Catalysis* 433 84
- [8] Yang J, Kikhtyanin O V, Wu W 2012 *Microporous and Mesoporous Materials* 150 14